


LETTER

Open Access



# Inertial focusing in a parallelogram profiled microchannel over a range of aspect ratios

Joo Young Kwon<sup>1</sup>, Dong-Ki Lee<sup>2</sup>, Jungwoo Kim<sup>1</sup> and Young Hak Cho<sup>1,2\*</sup> 

## Abstract

In this study, particle focusing phenomena are studied in parallelogram and rectangular cross-sectioned microchannels of varying aspect ratio. In contrast to prior work the microchannels were fabricated using anisotropic wet etching of a Si wafer, plasma bonding, and self-alignment between the Si channel and the PDMS mold. It is shown that the inertial focusing points of the fabricated microchannels of parallelogram and rectangular cross-section were modified as the aspect ratio of the microchannels changed. The particle focusing points of the parallelogram profiled microchannel are compared with those of the rectangular microchannel through experimental measurements and CFD simulation. It is shown that particles can be efficiently focused and separated at a relatively low Reynolds number using a parallelogram profiled microchannel with a low aspect ratio.

**Keywords:** Inertial focusing, Parallelogram microchannel, Anisotropic wet etching, Self-alignment, Aspect ratio

## Introduction

Over the last two decades, the application of microfluidic techniques has experienced rapid expansion in a vast range of fields, such as microelectronic cooling, MEMS (microelectromechanical systems), fuel cell technology, micro reactors for cell biology and tissue engineering, and medical and biomedical devices. Various transport phenomena in microchannels, which are indispensable elements in microfluidic devices, are widely studied. In particular, analytical studies on slip-flow, laminar flow and others have been conducted on microchannels with a range of cross section geometries, such as circular or rectangular cross-sections [1–3]. However, there are only experimental results for microchannels with a limited range of cross-sectional shapes as limitations in fabrication techniques mean research can only be conducted analytically.

Recent research has shown that there are many useful fluid inertia effects that are neglected in conventional microfluidics, which are available in a variety of

applications. Fluid inertia can be used for more efficient fluid mixing, particle separation, and focusing of biological cells [4–14]. Carlo presented focusing positions based on the cross-section shape of the microchannel, which are determined by the balance of the two inertial lift forces: the shear-gradient lift force and the wall-effect lift force [4]. Microchannels with a triangular and half-circular cross-section were fabricated to study inertial focusing of microparticles and manipulate them in non-rectangular cross-section channels [5]. Liu et al. conducted experiments and simulation to determine the complicated dependence of focusing behavior on particle size, channel aspect ratio, and the Reynolds number (Re). This provided physical insight into the multiplex focusing of particles in rectangular microchannels with different geometries and Reynolds numbers [6].

In this study, microchannels of parallelogram and rectangular cross-section were fabricated with various aspect ratios ( $AR = W/H$ , see Fig. 1) using the same fabrication method. Although both profiles had the same channel height, cross-section area and aspect ratio, they showed different behavior, especially at low aspect ratios. The focusing positions of particles in microchannels with parallelogram and rectangular cross-section were

\*Correspondence: yhcho@seoultech.ac.kr

<sup>1</sup> Department of Mechanical System Design Engineering, Seoul National University of Science & Technology, Seoul, South Korea  
Full list of author information is available at the end of the article

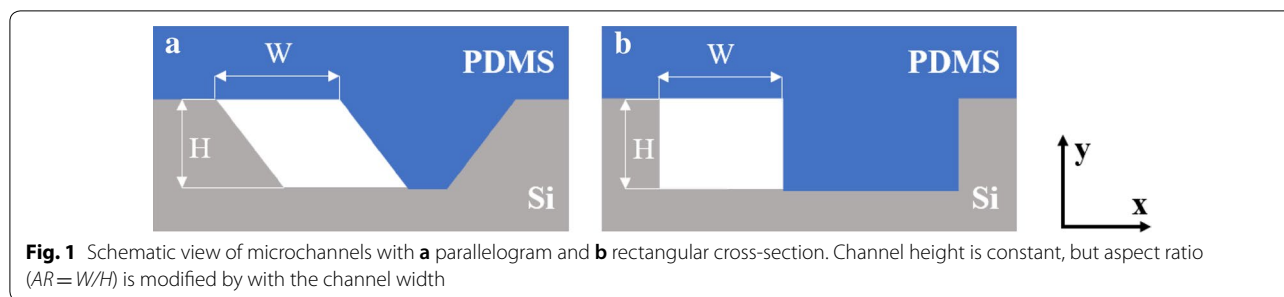


**Fig. 1** Schematic view of microchannels with **a** parallelogram and **b** rectangular cross-section. Channel height is constant, but aspect ratio ( $AR=W/H$ ) is modified by with the channel width

observed and analyzed according to  $AR$ . CFD (Computational Fluid Dynamics) simulations were conducted for the parallelogram profiled microchannel, which were compared with not only the experimental results, but also the simulation results for rectangular microchannels from a previous study [6].

### Experimental

In a previous study, microfluidic channels with various cross-sectional profiles, such as parallelogram, rhombus, pentagon and hexagon were fabricated [13]. In this study, photolithography, anisotropic wet etching, plasma bonding and self-alignment between the PDMS and Si were sequentially performed to fabricate microchannels having parallelogram and rectangular cross-sections with various  $AR$ s. Figure 1 shows a schematic view of microchannels with parallelogram and rectangular cross-sections fabricated using the same method. Both of these consisted of two Si surfaces and two PDMS surfaces, and had same channel height, cross-sectional area and  $AR$ . The height of the microchannels ( $H$ ) was fixed to 50  $\mu\text{m}$ , and their width ( $W$ ) was changed to fabricate the microchannels with various  $AR$ s. In this study, the reason why the rectangular microchannel was fabricated differently from the conventional rectangular microchannel fabrication process is that it provides a better comparison when composed of the same materials. In addition, this method has an advantage in that microchannels with various  $AR$ s can be easily fabricated when compared with the conventional fabrication method.

To study the effects of  $AR$ , microchannels with four different widths (50, 100, 150 and 250  $\mu\text{m}$ ), corresponding to four  $AR$  values (1, 2, 3 and 5 respectively), were fabricated. Polystyrene particles (10  $\mu\text{m}$ , green fluorescent, excitation 468 nm and emission 508 nm, Thermo SCIENCE Inc.) were dispersed in DI water (0.05~0.1 wt % concentration) with 1% Tween 20 (Sigma-Aldrich). The particle suspensions were then injected using a syringe pump (LEGATO 111, KD Scientific Inc.) with a controlled volumetric flow rate, and fluorescence microscopy (Leica DM IL LED and Leica EL6000, Leica

Microsystems Inc.) was used to confirm focusing positions in the microchannels.

### Simulation

To predict the equilibrium positions of the particles, the lift force of a particle in the parallelogram microchannel with  $AR=2$  was numerically calculated using the commercial CFD software ANSYS Fluent.

There are two approaches to investigate the mechanism of the particle migration/focusing: analytical and numerical simulation approaches. In the analytical approaches (for example, see Asmolov [7]), the inertial lift on the particle is estimated based on the point-particle based theory. However, for the particle with finite inertia, it is well known that applying the analytical approaches is limited because the point-particle based theory shows large deviation. Also, as mentioned by Liu et al. [6], for the three-dimensional microchannels considered in the study, the lift force is two-component vector in nature, but the theory is derived based on a plane channel. In these respects, the numerical approach is adopted to relieve the restriction of the analytical approach in the present study, which is similar to that described by Liu et al. [6].

Figure 2 shows schematics of a rigid spherical particle suspended in a microchannel with a parallelogram cross-section. As shown in Fig. 3, the cross-sectional area in each case is the same as that in the present experiment, and the axial length is also set to 1 mm for convenience of calculation. The total numbers of grid points considered are approximately 2 million and 3 million for  $AR=1$  and 2, respectively. In the calculation, the particle diameter ( $d$ ) is set to 9  $\mu\text{m}$ . The present grid resolution corresponds to  $\Delta/d=0.2$  relative to the particle diameter.

A uniform velocity condition ( $U_{in}=2$  m/s) is given to the inlet, which corresponds to  $Re (=U_{in} D_H/\nu_c)=90$  and 124 for  $AR=1$  and 2, respectively. Here,  $D_H$  is the hydraulic diameter of the parallelogram profiled microchannel and  $\nu_c$  is the kinematic viscosity of the working fluid.  $R_p=Re (d/D_H)^2=3.6$  and 2.6, respectively, for  $AR=1$  and 2. A uniform pressure condition was used at the outlet.

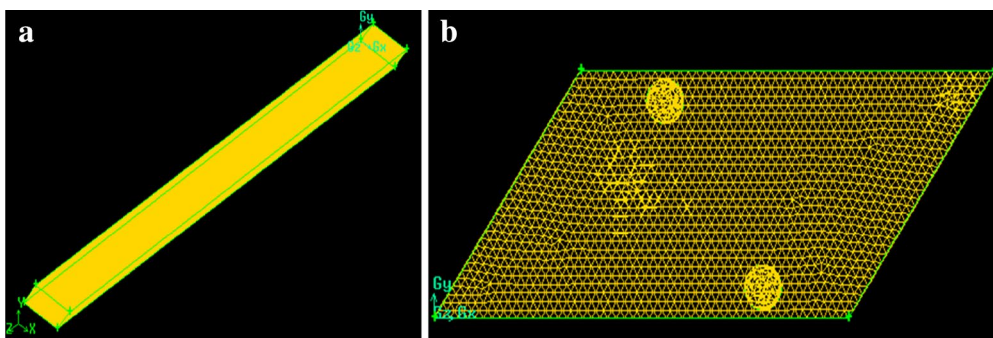


**Fig. 2** **a** Computational domain and **b** cross-sectional plane of a microchannel with a parallelogram profile of  $AR=2$

For the lift calculations, the particle is considered to be fixed at a specific position in the flow field. By changing the particle position, the variation of the lift force in the cross-sectional area could be estimated. Note that in the numerical simulation approach, the total lift force itself is directly obtained instead of its components (shear-gradient lift force and the wall-effect lift force). In the present study, therefore, the mechanism of the particle focusing is analyzed based on the magnitude and slope of the lift force as shown in “[Results and discussion](#)” section.

## Results and Discussion

In this study, microchannels with parallelogram and rectangular cross-sections, which had various  $AR$ s, were fabricated and then inertial focusing experiments were conducted. Figure 3 shows scanning electron microscope (SEM) images of microchannels with parallelogram and rectangular cross-sections. The height of the microchannels was fixed to  $50\ \mu\text{m}$ , and the widths used were  $50, 100, 150,$  and  $250\ \mu\text{m}$  ( $AR=1, 2, 3, 5,$  respectively). Therefore, because the cross-sectional areas of the microchannels were the same for each cross section, the Reynolds number was the same for a given flow rate. This enabled the change of the inertial focusing phenomena to be examined according to the change of the profile shape without the effect of the cross-sectional area.

The focusing behaviors of particles with diameters of  $10\ \mu\text{m}$  were experimentally observed in microchannels with  $AR$  values of  $1, 2, 3$  and  $5$ . Figure 4 shows fluorescence images of the particle distribution for the different microchannel shapes, and Fig. 5 shows the fluorescence intensities according to the particle position and cross-section shape. The fluorescence images in Fig. 4 were taken from top view, which was  $10\ \text{mm}$  away from the inlet of microchannel. The image data were acquired using optical microscope system equipped with a CCD camera and they were processed using image processing program (image J) (Fig. 5). The rectangular

microchannels showed particle distributions which were almost the same as those presented by Liu et al. [6]. However, the parallelogram profiled microchannels showed a very different particle distribution from that of the rectangular microchannels. In particular, when  $AR=1$  and the flow rate was  $18\ \text{ml/hr}$ , rectangular microchannels had four focusing points, but the parallelogram profiled microchannel had just two focusing points (as presented in a previous study [14]).

As shown in Figs. 4a and 5b, when  $AR=2$  there were four particle focusing points for the parallelogram, which were formed in oblique corners and in a central band. This result was similar to that of the particle distribution in a rectangular microchannel [6]. When the  $AR$  increased, the particle focusing points in the parallelogram microchannel increased from two to four and the position of the focusing points was different from that in a rectangular microchannel. It is believed that this was due to the dramatic change of the lift force with increasing  $Re$ .

The particles formed a wide band in the middle of the microchannels with  $AR=3$  and  $5$  for both microchannels. For microchannels with a high  $AR$  ( $AR=3$  and  $5$ ), a similar tendency of particle distribution was observed, which means that the effect of shape change decreased with increasing  $AR$ .

The CFD model predictions were compared to experimental measurements for parallelogram profiled microchannels with heights of  $50\ \mu\text{m}$  and widths of  $100\ \mu\text{m}$  in order to confirm the dependence of focusing behavior on the channel aspect ratio. Figure 6 shows the results of the  $x$ -directional force variation at several locations along  $y=6.25\ \mu\text{m}$ . As can be seen in Fig. 4, in the case of  $AR=1$ , the force exerted on the particle varies with a clear trend, but in the case of  $AR=2$ , there is a central plateau region. These results are thought to be related to the number of focusing points observed in the present experiment, which is qualitatively consistent with the

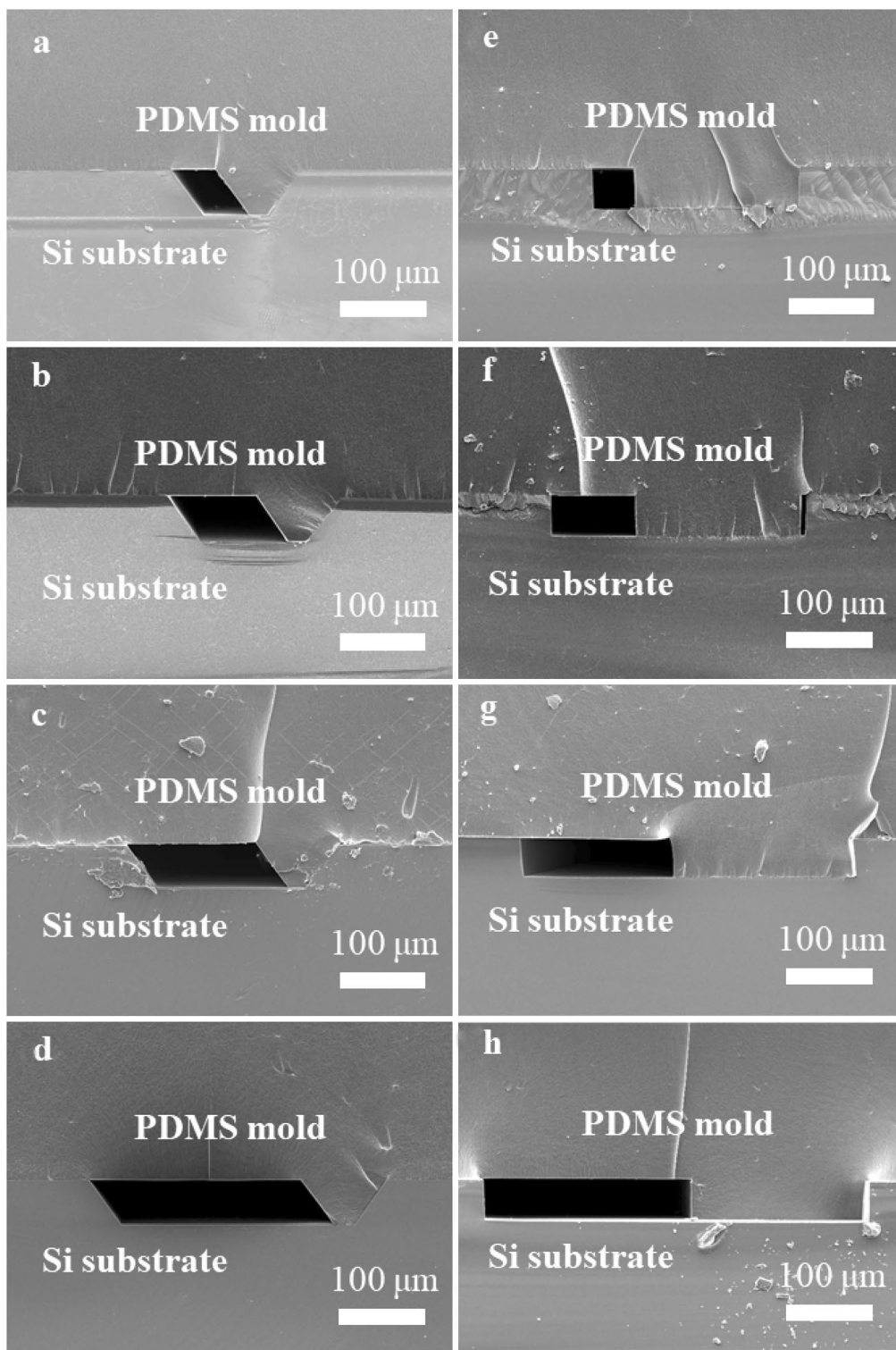


**Fig. 3** SEM images of microchannels with parallelogram and rectangular cross sections **a, b, c** and **d** AR = 1, 2, 3, 5 parallelogram profile microchannels, **e, f, g** and **h** AR = 1, 2, 3, 5 rectangular microchannels

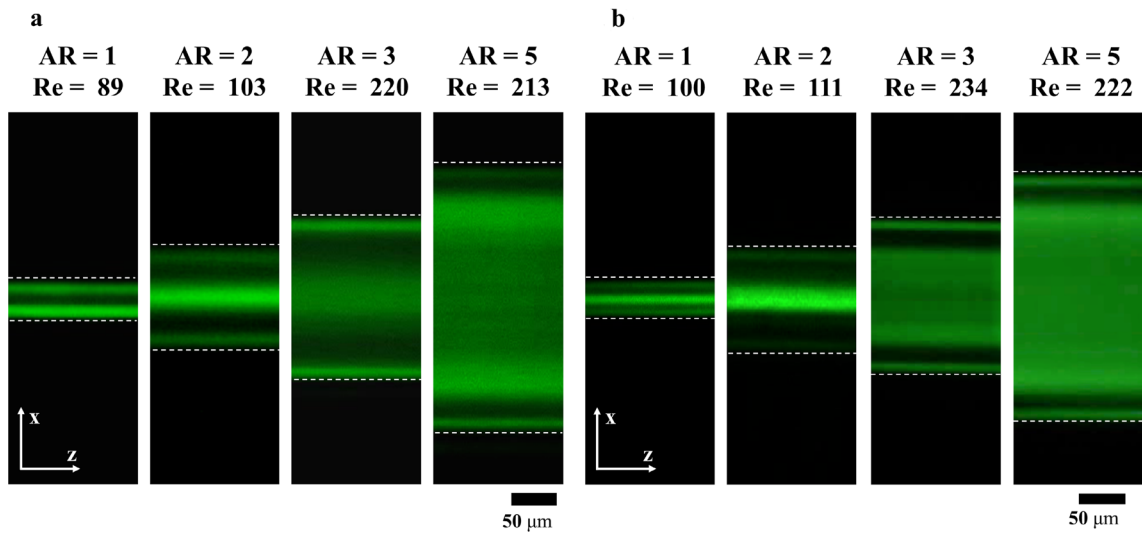


**Fig. 4** Fluorescence images of particle distribution for **a** parallelogram profiled microchannels, and **b** rectangular microchannels with  $AR = 1, 2, 3, 5$

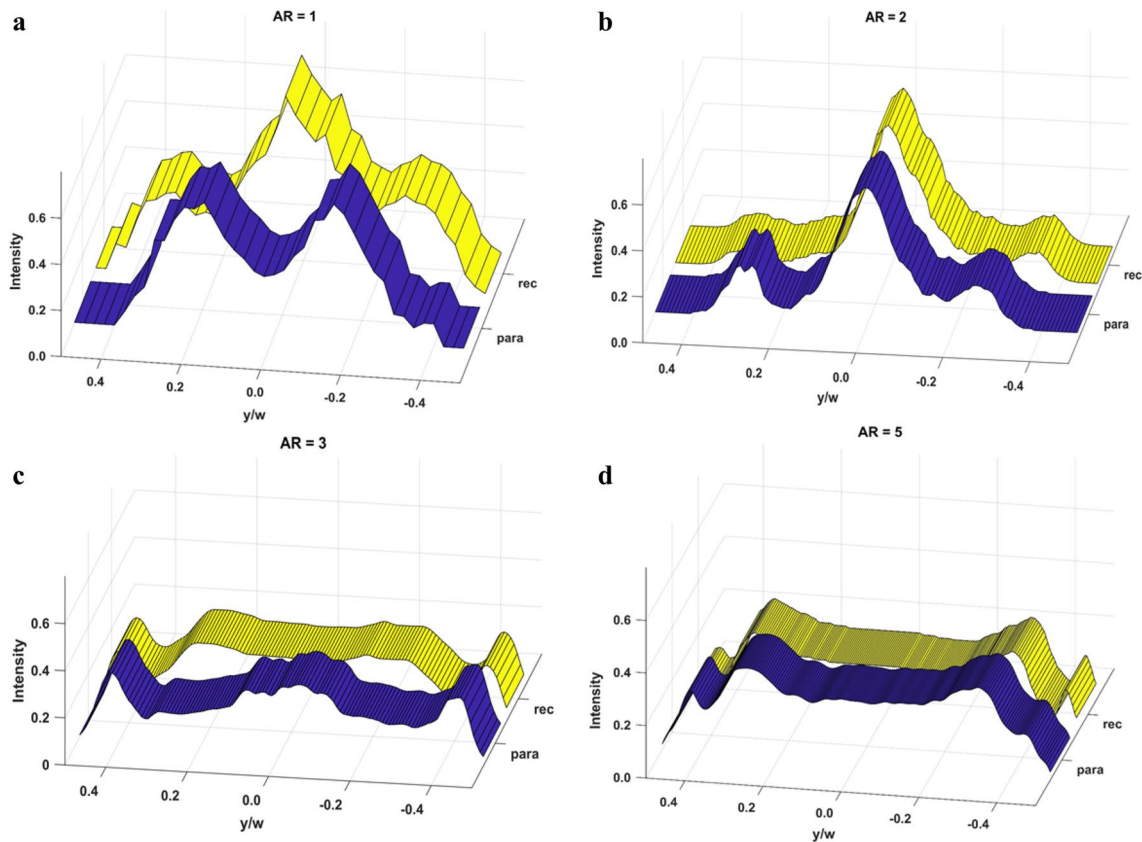
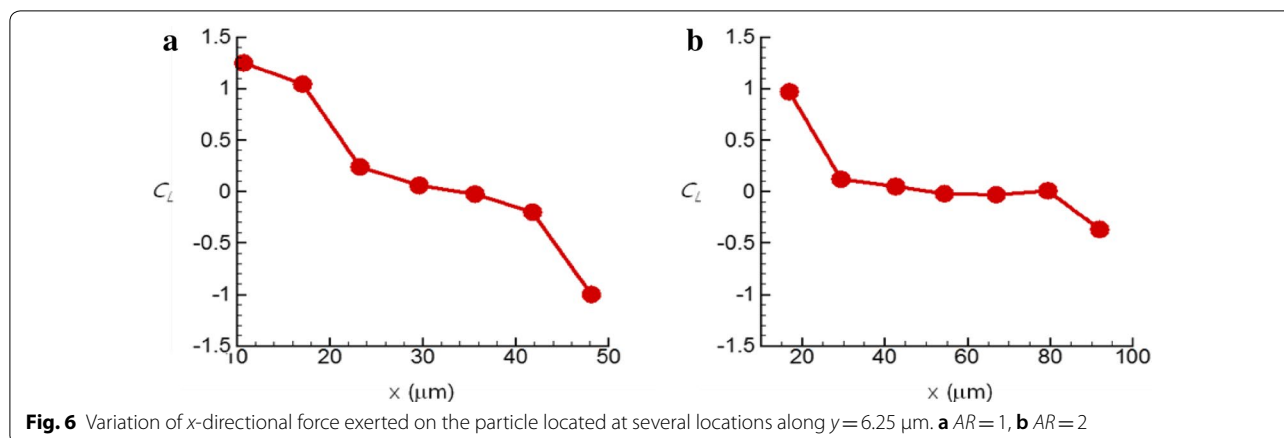


**Fig. 5** Fluorescence intensities (top view) according to the particle position and cross-section shape (yellow: rectangle, blue: parallelogram) for **a**  $AR = 1$ , **b**  $AR = 2$ , **c**  $AR = 3$ , **d**  $AR = 5$



results reported by Liu et al. [6]: one negative and two negative slopes. As mentioned by Liu et al., one and two negative slope cases correspond to one and two focusing points, respectively. Based on Liu et al.'s analysis, we expect that at the focusing point, the lift is close to zero and its slope is changed. In that respect, for  $AR=1$ , it is found that the focusing point exists at around  $x=30 \mu\text{m}$ . On the other hand, for  $AR=2$ , they exist at around  $x=30$  and  $80 \mu\text{m}$ . For further understanding, the pressure and viscous contributions to the force were examined. For the case of  $AR=1$ , the pressure contribution is dominant over the viscous one, which might be explained by the confined wall effect. On the other hand, for the case of  $AR=2$ , the viscous contribution exceeds that of the pressure. As a result, the different contributions of the pressure and viscous forces for  $AR=1$  and 2 result from the variations of total force as shown in Fig. 6.

## Conclusions

In the present study, microchannels having parallelogram and rectangular cross-sections with various  $AR$ s were fabricated, and the particle focusing phenomena were compared using fluorescent particle flows. For  $AR=1$ , the rectangular channel had four focusing points, which were located at the center of each plane, while the parallelogram profiled channel had two focusing points. As  $AR$  increased, the focusing positions changed and finally both geometries exhibited a similar particle distribution. Simulation results for parallelogram microchannels explained that the different contributions of the pressure and viscous forces for  $AR=1$  and 2 would result from the different distributions of the total force, so a different number of particle focusing points were displayed. From these results, it is expected that it will be possible to efficiently separate the particles at relatively low Reynolds

number using a parallelogram profiled channel with a low aspect ratio.

## Abbreviations

$AR$ : aspect ratio;  $W$ : width of microchannel;  $H$ : height of microchannel;  $\Delta$ : mesh size;  $d$ : particle diameter;  $U_{in}$ : inlet bulk velocity;  $D_{H}$ : hydraulic diameter of microchannel;  $\nu_c$ : kinematic viscosity of working fluid;  $Re$ : Reynolds number;  $R_p$ : particle Reynolds number.

## Acknowledgements

This work was supported by the National Research Foundation of Korea (NRF) Grant funded by the Korean government (MSIP) (No. NRF-2017R1D1A1B03029817).

## Authors' contributions

JYK carried out the experiments and analyzed the experimental results. JK carried out and analyzed the CFD simulation. DK, JK and YHC discussed the experimental result. JK and YHC drafted the manuscript. All the authors discussed the experimental and simulation results. All authors read and approved the final manuscript.

## Funding

This work was supported by the National Research Foundation of Korea (NRF) Grant Funded by the Korean government (MSIP) (No. NRF-2017R1D1A1B03029817).

## Availability of data and materials

Not applicable.

## Competing interests

The authors declare that they have no competing interests.

## Author details

<sup>1</sup> Department of Mechanical System Design Engineering, Seoul National University of Science & Technology, Seoul, South Korea. <sup>2</sup> Institute of Precision Machinery Technology, Seoul National University of Science & Technology, Seoul, South Korea.

Received: 5 September 2019 Accepted: 13 December 2019

Published online: 20 December 2019

## References

1. Tamayol A, Bahrami M (2010) Laminar flow in microchannels with noncircular cross section. *J Fluid Eng* 132:111201
2. Tamayol A, Hooman K (2011) Slip-flow in microchannels of non-circular cross sections. *J Fluid Eng* 133:091202

3. Sadeghi M, Sadeghi A, Saidi MH (2016) Electroosmotic flow in hydrophobic microchannels of general cross section. *J Fluid Eng* 138:031104
4. Di Carlo D (2009) Inertial microfluidics. *Lab Chip* 9:3038–3046
5. Kim J, Lee J, Wu C, Nam S, Di Carlo D (2016) Inertial focusing in non-rectangular cross-section microchannels and manipulation of accessible focusing positions. *Lab Chip* 16:992–1001
6. Liu C, Hu G, Jiang X, Sun J (2015) Inertial focusing of spherical particles in rectangular microchannels over a wide range of Reynolds numbers. *Lab Chip* 15:1168–1177
7. Asmolov ES (1999) The inertial lift on a spherical particle in a plane Poiseuille flow at large channel Reynolds number. *J Fluid Mech* 381:63–87
8. Bhagat AAS, Kuntaegowdanahalli SS, Papautsky I (2009) Inertial microfluidics for continuous particle filtration and extraction. *Microfluid Nanofluid* 7:217–226
9. Yuan C, Pan Z, Wu H (2018) Inertial migration of single particle in a square microchannel over wide ranges of Re and particle sizes. *Microfluid Nanofluid* 22:102
10. Gou Y, Jia Y, Wang P, Sun C (2018) Progress of inertial microfluidics in principle and application. *Sensors* 18:1762
11. Maseeli M, Sollier E, Amini H, Mao W, Camacho K, Doshi N, Mitragotri S, Alexeev A, Di Carlo D (2012) Continuous inertial focusing and separation of particles by shape. *Phys Rev X* 2:031017
12. Wu Z, Chen Y, Wang M, Chung AJ (2016) Continuous inertial microparticle and blood cell separation in straight channels with local microstructures. *Lab Chip* 16:532–542
13. Chung AJ, Gossett DR, Di Carlo D (2013) Three Dimensional, sheathless, and high throughput microparticle inertial focusing through geometry induced secondary flows. *Small* 9:685–690
14. Lee D, Kwon JY, Cho YH (2019) Fabrication of microfluidic channels with various cross-sectional shapes using anisotropic etching of Si and self-alignment. *Appl Phys A* 125:291

### Publisher's Note

Springer Nature remains neutral with regard to jurisdictional claims in published maps and institutional affiliations.

Submit your manuscript to a SpringerOpen<sup>®</sup> journal and benefit from:

- Convenient online submission
- Rigorous peer review
- Open access: articles freely available online
- High visibility within the field
- Retaining the copyright to your article

---

Submit your next manuscript at ► [springeropen.com](https://www.springeropen.com)

---